Precipitation as the main mechanism for Cd(II), Pb(II) and Zn(II) removal from aqueous solutions using natural and activated forms of red mud

Fabiano Tomazini da Conceição, Mariana Scicia Gabriel da Silva, Amauri Antonio Menegário, Maria Lucia Pereira Antunes, Guillermo Rafael Beltran Navarro, Caetano Dorea, … & Rodrigo Braga Moruzzi

July 2021

Environmental Advances 4 (2021) 100056

Contents lists available at ScienceDirect

Environmental Advances

journal homepage: www.elsevier.com/locate/envadv

Precipitation as the main mechanism for Cd(II), Pb(II) and Zn(II) removal from aqueous solutions using natural and activated forms of red mud

Fabiano Tomazini da Conceição[a,*], Mariana Scicia Gabriel da Silva[a], Amauri Antonio Menegário[b], Maria Lucia Pereira Antunes[c], Guillermo Rafael Beltran Navarro[a], Alexandre Martins Fernandes[a], Caetano Dorea[d], Rodrigo Braga Moruzzi[a]

[a] Instituto de Geociências e Ciências Exatas, UNESP - Universidade Estadual Paulista, 1 – Avenida 24-A, n° 1515, C. P. 178, CEP 13506-900, Bela Vista, Rio Claro, São Paulo, Brazil
[b] Centro de Estudos Ambientais, UNESP - Universidade Estadual Paulista, Rio Claro, Brazil
[c] Instituto de Ciência e Tecnologia, UNESP - Universidade Estadual Paulista, Sorocaba, Brazil
[d] Department of Civil Engineering, University of Victoria, Victoria, Canada

ARTICLE INFO

Keywords:
Brazilian red mud
Trace elements
Sequential extraction
Kinetics modelling

ABSTRACT

The red mud (RM) has been used as an alternative low-cost adsorbent to remove trace elements, with the adsorption onto sodalite surface described as the main removal mechanism for trace elements. However, recent studies have shown that precipitation might be of great importance for some trace metals removal using natural and thermal activated RM. Therefore, the aim of this study was to identify the main mechanism responsible for Cd(II), Pb(II) and Zn(II) removal from aqueous solutions using natural and activated forms of RM, based on sequential extractions and a precipitation kinetic model was developed. Results showed that the carbonate fraction was responsible for the highest trace elements removal (ca. 85%), with the minerals assemblages precipitated: otavite – $CdCO_3$, cerussite - $PbCO_3$, smithsonite - $ZnCO_3$ and anglesite - $PbSO_4$. The kinetic model showed that the mineral precipitation was limit due to the HCO_3^- consumption during the formation of new minerals. Hence, this study showed that precipitation was the central mechanism on trace elements removal, regardless the natural or activated forms of RM. This finding raise doubt about the effectiveness of the traditional adsorption isotherms and kinetics models to describe trace metals removal using RM, contributing with new insights for future researches involving these hazardous materials.

1. Introduction

Brazilian mining activities contribute significantly to global mineral production, including the third-largest global production of bauxite (Brasil, 2018). Brazil benefited more than 35 megatons of bauxite via the Bayer Process®, generating a residue known as bauxite residue or red mud – RM (Hind et al., 1999). According to Fortes et al. (2016), about 10–25 million tons/year of RM are generated in Brazil. The Brazilian RM can be considered a hazardous material due to presence of different oxides and toxic trace elements mixed in a highly alkaline matrix (Antunes et al., 2012; Souza et al., 2013). The disposal of this residue usually occurs in tailing dams, producing a high financial and environmental cost, leading to problems related to contamination of soil, groundwater and surface water and damage to flora and fauna (Silva Filho et al., 2007; Jones and Haynes, 2011). The main accident involving the rupture of the RM tailing dam was in October 2010 in Ajka (Hungary), causing 10 deaths and more than 100 injuries (Hua et al., 2017). In Brazil, an environmental disaster caused by high rainfall occurred in a RM tailing dam located in Barbacena (Pará State) in February 2018, affecting thirteen riverside communities, which depends on the natural resources of the Pará River basin in this municipality (Amazônia Real, 2018).

Cadmium – Cd(II), lead - Pb(II) and zinc – Zn(II) are commonly used in several human activities, such as mining, smelting, electroplating, dyes, ceramics, among others. These trace elements are not compatible with biological treatment processes, and adsorption is the main technique for these trace elements removal in the treatment of industrial effluents (Nadaroglu et al., 2010). The Cd(II) causes vomiting and lung and kidney diseases, with the Pb(II) affecting almost all organs, with the central nervous system being the most sensitive, while the Zn(II) can causes vomiting, anaemia and kidney and liver damage (São Paulo, 2012). RM has been used for Cd(II), Pb(II) and Zn(II) removal, with application of the natural (Vaclavikova et al. 2005; Santona et al. 2006; Pichinelli et al., 2017; Ayala and Fernández 2019; Silva et al., 2019) or activated (Apak et al. 1998a 1998b;

* Corresponding author.
E-mail address: fabiano.tomazini@unesp.br (F.T. da Conceição).

https://doi.org/10.1016/j.envadv.2021.100056
Received 4 March 2021; Received in revised form 2 April 2021; Accepted 12 April 2021

Table 1
Studies of Cd(II), Pb(II) and Zn(II) removal (mmol g^{-1}) from aqueous solutions using natural red mud (RM) and with different activations procedures.

Metal	Natural and activated forms	Removal	Reference
Cd(II)	RM	0.26	Ayala and Fernández (2019)
	RM	0.87	Silva et al. (2019)
	RM	1.41	Vaclavikova et al. (2005)
	RM	1.35	Santona et al. (2006)
	RM - heated	1.04	Silva et al. (2019)
	RM - heated	0.27	Gupta and Sharma (2002)
	RM - heated	0.38	Yang et al. (2020)
	RM - HCl	0.95	Santona et al. (2006)
	RM –HCl	0.14	Silva et al. (2019)
	RM - HCl	2.24	Apak et al. (1998a)
	RM - $CaSO_4$	0.22	Lopez et al. (1998)
	RM - $Ca(NO_3)_2$	0.68	Silva et al. (2019)
Pb(II)	RM	2.13	Pichinelli et al. (2017)
	RM	1.88	Santona et al. (2006)
	RM - heated and H_2O_2	0.35	Gupta et al. (2001)
	RM - carbonised	0.45	Pulford et al. (2012)
	RM - HCl	0.77	Santona et al. (2006)
	RM - HCl	0.84	Apak et al. (1998a)
	RM - $Ca(NO_3)_2$	2.23	Pichinelli et al. (2017)
	RM – colloidal silica and NaOH	2.66	Lyu et al. (2020)
	RM	0.18	Ayala and Fernández (2019)
Zn(II)	RM	1.14	Pichinelli et al. (2017)
	RM	2.47	Santona et al. (2006)
	RM	2.05	Vaclavikova et al. (2005)
	RM - heated	0.22	Gupta and Sharma (2002)
	RM - HCl	1.59	Santona et al. (2006)
	RM - $CaSO_4$	0.19	Lopez et al. (1998)
	RM - $Ca(NO_3)_2$	0.96	Pichinelli et al. (2017)
	RM - CO_2	0.23	Sahu et al. (2011)

Lopez et al. 1998; Gupta et al. 2001; Gupta and Sharma 2002; Santona et al. 2006; Silva et al., 2019; Sahu et al. 2011; Pulford et al., 2012; Pichinelli et al., 2017; Silva et al., 2019; Lyu et al., 2020) forms of RM. All studies present in Table 1 have been associated to the adsorption of these trace elements onto the RM surface, and the adsorption was modelled using Langmuir and Freundlich isotherms. Sodalite pointed out as the main responsible for the Cd(II), Pb(II) and Zn(II) adsorption in natural and activated forms of RM (Santona et al., 2006; Pichinelli et al., 2017; Silva et al., 2019). In addition, different kinetics models were applied to describe the adsorption processes, such as the pseudo-first-order, the pseudo-second-order, the Elovich and the intra-particle diffusion models.

The trace elements adsorption onto sodalite is associated to ion exchangeable and, consequently, the use of sequential extractions can be a useful tool to confirm this mechanism. Tessier et al. (1979) proposed a method for sequential extraction to identify the geochemical fractions. This method assesses the potential mobility for trace elements, showing the labile (ion exchangeable, bound to carbonates, bound to Fe-Mn oxides and bound to organic matter/sulfide) and residual phases. Recent studies using sequential extraction have reported that the Cu(II) (Qi et al., 2018) and Cr(II) (Qi et al., 2020) removal in RM were preferably associated with bound to carbonate and bound to Fe-Mn oxides, respectively, instead of adsorption in ion exchangeable. Yang et al. (2020) proposed the Cd(II) removal is associated to adsorption in bound to Fe-Mn oxides rather than adsorption (in ion exchangeable) when thermal treated RM was studied. Lyu et al. (2020) applied adsorption isotherms to describe adsorption of Pb(II) onto RM modified by colloidal silica and sodium hydroxide; however, the authors have concluded that the precipitation processes was responsible for 78% of Pb(II) removal, as Pb-carbonates, even no specific analysis was performed.

Taking into account the recent findings on trace elements removal mechanisms using RM, the role of precipitation should be thoroughly developed and the use of adsorption models to describe trace elements removal reconsidered. The few studies using sequential extractions are limited to Cu(II) and Cr(II) removal by natural RM (Qi et al., 2018, 2020, respectively) and Cd(II) removal by thermal activated forms of RM (Yang et al., 2020), and they have shown the removal precipitations products only, with no precipitation kinetics model proposed. Thus, the main aim of this study was to determine the central mechanism responsible for Cd(II), Pb(II) and Zn(II) removal using natural and activated forms of RM (heated at 400°C - RM_{400} and with chemical treatments using HCl - RM_{HCl} and $Ca(NO_3)_2$ - RM_{Ca}), applying the sequential extraction method. Secondary, a kinetic model was performed to describe the time effect on the Cd(II), Pb(II) and Zn(II) removal and to determine the precipitation kinetic constants and the reaction order. Therefore, this paper expands the understanding and provide new insight into the interactions mechanisms among Cd(II), Pb(II) and Zn(II) and these hazardous materials, which can be used as low-cost material in the field of environmental remediation and water industry.

2. Materials and methods

2.1. Sampling and activation procedures

The municipality of Alumínio (Fig. 1a), São Paulo State, Brazil, hosts the main aluminium plant in Brazil, where the natural RM was sampled (June – 2017) in a tailing dam (Fig. 1b). The RM was dried for 12 h at 50 °C. Antunes et al. (2012) studied the thermal behavior and physical properties of RM from Brazil (from 400 to 800 °C) and concluded that the best temperature to produce RM with a large surface area is 400 °C due to phase transition of goethite to hematite and gibbsite to alumina. Thus, the RM was heated in a muffle furnace oven at 400 °C for two hours (RM_{400}) to increase the removal capacity in relation to natural RM (Antunes et al., 2012). The RM with chemical treatments (HCl - RM_{HCl} and $Ca(NO_3)_2$ - RM_{Ca}) were performed to promote the extraction of the exchangeable phase by means of the desorption on the RM surface (Santona et al., 2006; Pichinelli et al., 2017). For the chemical activation, RM was mixed either with 0.05 mol L^{-1} HCl or with 0.1 mol L^{-1} $Ca(NO_3)_2$ (1 g:25 mL) and agitated for 2 h. The supernatant was re-

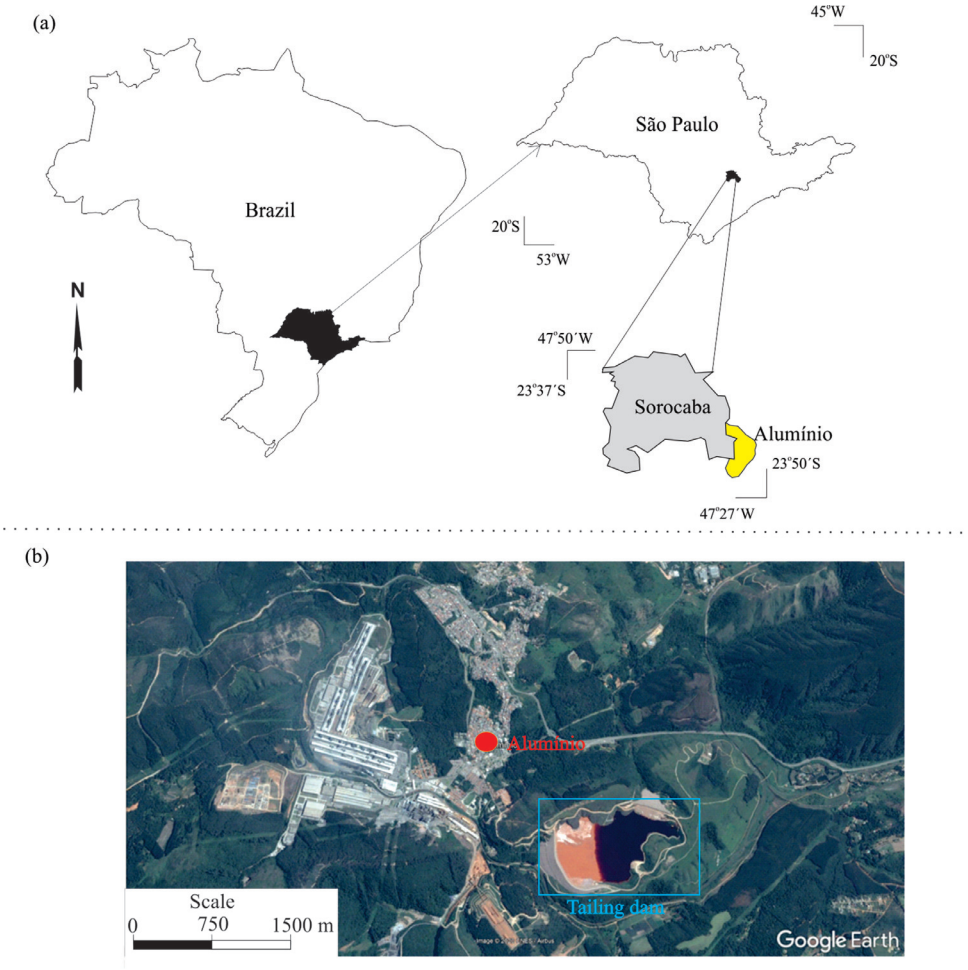

Fig. 1. Location of Alumínio in the São Paulo State (a). The aluminium plant and tailing dam, with the image from Google Earth Pro - 04/10/2020 (b).

moved and the RM_{HCl} and RM_{Ca} samples were washed three times, using ultrapure water with electrical conductivity lower than 0.02 μS cm^{-1} and, then, dried at 50 °C for 12 h.

2.2. Characterization of natural and activated forms of RM

The pH values for RM, RM_{400}, RM_{HCl} and RM_{Ca} in solution were characterized using 1 g:25 mL of ultrapure water, using YSI 556 Multi-Probe System calibrated with pure standards at pH 4 and 7. The specific surface area (SSA) for the RM, RM_{400}, RM_{HCl} and RM_{Ca} samples were determined by BET method, using a Micromeritics ASAP Tristar 3000 analyser operated at -196 °C calibrated with nitrogen adsorption curves.

The pH_{PCZ} is another important issue on Cd(II), Pb(II) and Zn(II) removal by RM, once it determines whether electrostatic attraction or respulsion between the sorbents and sorbates (Orfão et al., 2006; Jesus et al., 2015). The point of zero charge (pH_{PZC}) value of RM, RM_{400}, RM_{HCl} and RM_{Ca} was characterized using a mixed of 0.1 g of these materials with 20 mL of 0.1 mol L^{-1} NaCl at initial pH varying from 1 to 11 (Jesus et al., 2015). The solution was shaken at 250 1rpm at 25 °C for 24 h, and then the final pH was measured. Initial and final pH values were plotted and the pH_{PZC} value was determined according to Orfão et al. (2006).

In order to identify the minerals in the RM, RM_{400}, RM_{HCl}, RM_{Ca} and control samples, the X-ray diffractometry (XRD – PANalytical Empyrean Instrument) was used on powdered samples from 2° to 90° with 0.02° step-sizes, operating at 40 kV and 40 mA, with CuKα radiation. The mineralogical identification was performed by the software X'Pert Highscore Plus®, using ICDD PDF2 database. The morphology of all samples was identified using a Scanning Electron Microscope with an Energy Dispersive X-ray Spectrometer (SEM-EDS, JEOL JSM-6010LA).

2.3. Removal experiment

The Cd(II), Pb(II) and Zn(II) aqueous solutions (25 mL), with the initial concentration of 80 mmol L^{-1}, were mixed with 1.0 g of RM, RM_{400}, RM_{HCl} and RM_{Ca}. The solutions of Cd(II), Pb(II) and Zn(II) were prepared using analytical grade nitrate salts: $Cd(NO_3)_2.4H_2O$, $Pb(NO_3)_2$ and $Zn(NO_3)_2.6H_2O$. The samples were stirred at 145 rpm at 25 °C for 12 h and then centrifuged for 25 min at 3000 rpm. Afterwards, the RM, RM_{400}, RM_{HCl} and RM_{Ca} samples were dried for 12 h at 50 °C. Silva et al. (2019) and Pichinelli, et al. (2017) studied the influence of pH (2, 4, 7, 10 and 12) on the Cd(II) and Pb(II) and Zn(II) removal. The authors showed the pH 7 as the best value for removal of these trace elements, although the pH raging between 5.0 and 5.5 have been widely used (Santona et al., 2006; Nadaroglu et al., 2010, Smiljamic et al., 2010, Smiciklas et al., 2014; Conceição et al., 2016). Thus, all the experiments for trace elements removal analysis were performed at initial pH of 7, with the final pH values characterized at 5.

2.4. Sequential extraction

The sequential extraction in RM, RM_{400}, RM_{HCl} and RM_{Ca} was applied as described by Tessier et al. (1979) and Leleyter and Probst (1999). The detailed sequential extraction procedure is presented in Table 2, with two different geochemical fractions: labile (F1 – ion exchangeable, F2 – bound to carbonate, F3 – bound to Fe-Mn oxides and F4 – bound to organic matter/sulfide) and residual (F5). After each extraction step, the samples were centrifuged at 3000 rpm for 25 min. at 25 °C. Once finished, the residual RM, RM_{400}, RM_{HCl} and RM_{Ca} were dried at 25 °C and applied for the next steps. The percentage (*P*) of Cd(II), Pb(II) and Zn(II) due to sequential extraction in RM, RM_{400}, RM_{HCl} and RM_{Ca}

Table 2
Sequential extraction protocols.

Step	Fraction	Protocols
F1	Ion exchangeable	10 mL of $MgCl_2$ 0.5 M for 2 h at 25 °C and pH 5.5
F2	Bound to Carbonate	10 mL of CH_3COONa 1 M for 5 h at 25 °C and pH 4.5
F3	Bound to Fe-Mn oxides	10 mL of $NH_2OH.HCl$ 0.04 M in 25% (v/v) acetic acid for 5 h at 85 °C and pH 2.5–3.0
F4	Bound to organic matter/sulfide	3 mL of HNO_3 0.02 M + 8 mL of H_2O_2 35% for 5 h at 85 °C and pH 2.0. After cooling to 25 °C, it was added 20 mL of ammonium acetate 0.85 M in 5% (v/v) HNO_3 for 30 min
F5	Residual	digestion procedure following the EPA 3010A (USEPA, 1990)

was calculated using the Eq. (1).

$$P_j\ (\%) = \frac{[F_j]}{\sum_{i=1}^{5}[Fi]}\ .100 \quad \text{for } j = 1,2..5 \tag{1}$$

where:

P = percentage of each geochemical fraction for Cd(II), Pb(II) or Zn(II); $[F]$ = Cd(II), Pb(II) and Zn(II) concentration in each geochemical fraction (mmol g^{-1}); Indexes j and i = geochemical fraction in which P is calculated over all extracted forms, respectively.

2.5. Kinetics studies

The kinetics studies were carried out using 1 g (m): 25 mL (V) of an aqueous solution, with the Cd(II), Pb(II) and Zn(II) initial concentrations of 80 mmol L^{-1} (C_0). The samples were stirred at 145 rpm, removed after 15, 30, 60, 120, 420, 660 and 1440 min, centrifuged at 3000 rpm for 25 min at 25 °C, with the supernatant separated and the residual Cd(II), Pb(II) and Zn(II) measured (C_f). The initial pH (t = 0 min) was adjusted to 7 as explained above, with the final pH characterized at 5 after 1440 min. The Eqs. (2) and (3) represent the amount of Cd(II), Pb(II) and Zn(II) retained (A_S - mmol g^{-1}) and the removal efficiency in all experiments (RE - %), respectively. After confirming the dominant mechanism of Cd(II), Pb(II) and Zn (II) removal, the kinetic model for trace metals precipitation was performed as described in detail at Section 3.4.

$$A_s = (C_0 - C_f).\frac{V}{m} \tag{2}$$

$$RE = \frac{C_0 - C_f}{C_0}\ .100 \tag{3}$$

2.6. Analysis

The supernatants associated to sequential extraction and kinetics studies were then transferred to a Teflon tube of 50 mL, made up to volume with ultrapure water, for analysis of the Cd(II), Pb(II) and Zn(II) concentrations by inductively coupled plasma optical emission spectrometry (ICP OES), iCAP 6000 SERIES machine Thermo Scientific. The detection limit was 0.006 mg L^{-1} for all trace elements. All experiments were carried out in triplicate.

3. Results and discussion

3.1. Characterisation of RM, RM_{400}, RM_{HCl} and RM_{Ca}

The pH values for the RM, RM_{400}, RM_{HCl} and RM_{Ca} in solution were 10.5, 10.7, 8.3 and 7.5, respectively. The thermal treatment did not change the pH values in relation to RM. However, the pH values after the chemical treatment were lower than the RM due to CO_3^{2-} consumption during the reactions of CO_3^{2-} present in the RM, water and HCl or $Ca(NO_3)_2$ (Santona et al., 2006; Pichinelli et al., 2017). The pH_{PCZ} values were for 8.8, 8.3, 9.1 and 9.9 for RM, RM_{400}, RM_{HCl} and RM_{Ca}, respectively. The thermal treatment increased the specific surface area (SSA) in RM_{400} in relation to RM (from 33 to 61 $m^2\ g^{-1}$), while the chemical treatment decreased the SSA values (25 and 27 $m^2\ g^{-1}$ to RM_{HCl} and RM_{Ca}, respectively).

Fig. 2 shows the XRD patterns with the minerals found in the RM, RM_{400}, RM_{HCl} and RM_{Ca} samples. The RM is composed of kaolinite ($Al_2Si_2O_5(OH)_4$), gibbsite ($Al(OH)_3$), sodalite ($Na_8Al_6Si_6O_{24}Cl_2$), goethite (FeO(OH)), quartz (SiO_2) and calcite ($CaCO_3$). However, after the thermal treatment, the peaks caused by aluminum and iron hydroxides were not detected from the RM_{400} XRD patterns. This can be explained by the conversion of goethite to hematite at 243 °C and also by the fact that the gibbsite is transformed to transition aluminas (χAl_2O_3) at 272 °C (Antunes et al., 2012). The RM_{HCl} and RM_{Ca} presents the same minerals described for the RM. The morphology of RM, RM_{400}, RM_{HCl}

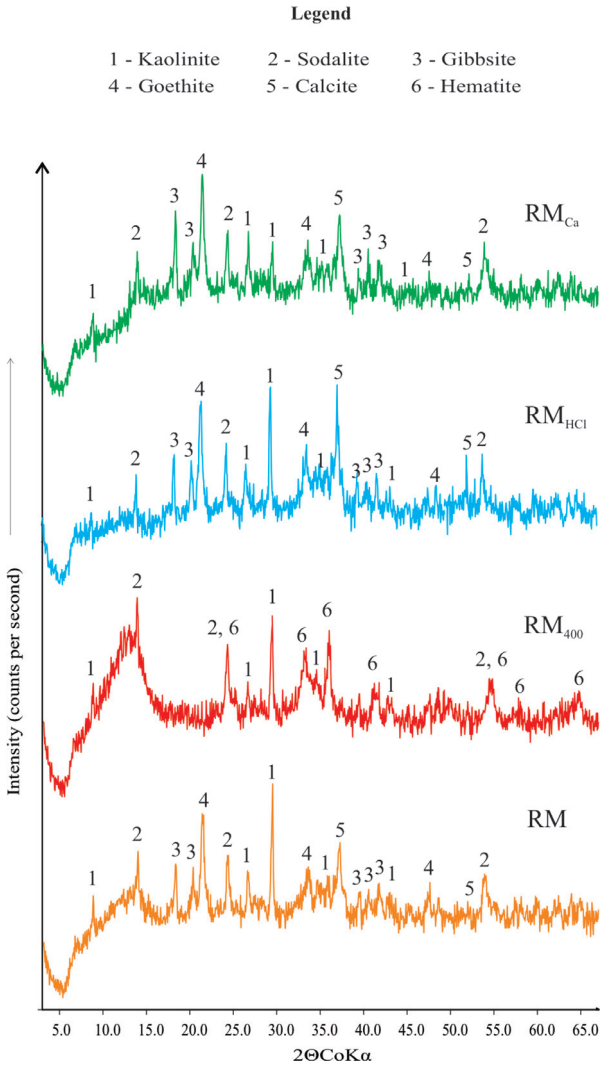

Fig. 2. XRD patterns of RM, RM_{400}, RM_{HCl} and RM_{Ca}.

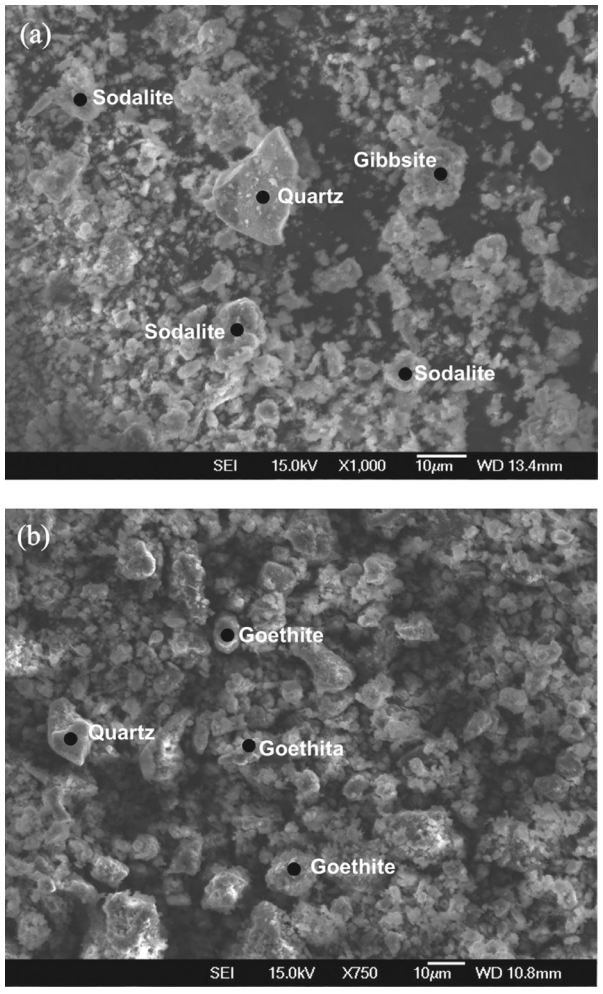

Fig. 3. SEM images of RM.

and RM_{Ca} particles was observed by SEM-EDS. Particles of different size, shape and texture were observed in RM sample, as illustrated in Fig. 3. Heterogeneous materials with particle diameters between from < 1 μm to > 10 μm can be seen. It can be observed that the chemical or thermal treatment did not alter the mineral morphology, with the smallest particles corresponding to iron oxides and the largest ones to silicon.

3.2. Sequential extractions

The percentages of labile and residual geochemical fractions of Cd(II), Pb(II) and Zn(II) in the RM, RM_{400}, RM_{HCl} and RM_{Ca} samples are present in Fig. 4. By the analysis of trace elements in the geochemical fractions, it is possible to note that the labile geochemical fractions were responsible for ca. 95% of these trace elements, as 6.0 ± 0.3% for Cd(II); 3.5 ± 0.3% for Pb(II) and 7.3 ± 0.4% for Zn(II) are associated to residual fraction. The lowest concentrations for Cd(II), Pb(II) and Zn(II) were measured in the ion exchangeable fraction (< 0.4% for all trace elements) in comparison to other labile geochemical fractions, with a maximum removal of 0.04, 0.06 and 0.04 mmol g^{-1} for Cd(II), Pb(II) and Zn(II), receptively.

Sodalite is a tectosilicate considered as zeolite-type and it has been considered the main responsible for the Cd(II), Pb(II) and Zn(II) adsorption in natural and activated RM (Santona et al., 2006; Silva et al., 2019; Yang et al., 2020). Unfortunately, the pH_{PCZ} of sodalite has not been characterised yet, but it has been advised that the negatively-charged surface can be neutralized by the adsorption of Cd(II), Pb(II) and Zn(II) within the outer-sphere bonds and in the cages and channels of its framework (Whittington et al., 1998; Mon et al., 2005). However, the low Cd(II), Pb(II) and Zn(II) percentages in the ion exchangeable fraction clearly indicate that these trace elements removal by natural and activated forms of RM cannot be only explained by the trace metals adsorption onto sodalite.

The Cd(II), Pb(II) and Zn(II) bound to Fe-Mn oxides and bound to organic matter/sulfide were 7.9 ± 0.3%, 4.3 ± 0.2% and 0.4 ± 0.1%, 2.8 ± 0.2% and 0.6 ± 0.2%, respectively. Qi et al. (2020), showed that the main Cr(II) removal processes in the RM collected from Shanxi in China was the bound to Fe-Mn oxides. Yang et al. (2020) suggested that the Fe-Mn oxides were responsible for Cd(II) removal from aqueous solution, instead carbonate precipitation, due to low content of total inorganic carbon present in the RM with heat treatment ranging from 200 to 900°C sampled in the north of China. The Cd(II), Pb(II) and Zn(II) removal in the Fe-Mn oxides is due to adsorption onto goethites and hematites present in the natural and activated RM, which have large specific surface area and reactive -OH and $-OH_2$ functional groups exposed on their surface (Liu and Huang, 2003). In addition, these trace elements also can be adsorbed onto oxides and hydroxides of Al^{3+} through the formation of inner-sphere bounds (Santona et al., 2006).

The carbonate fraction was the labile fraction responsible for the higher Cd(II), Pb(II) and Zn(II) removal percentages in the RM, RM_{400}, RM_{HCl} and RM_{Ca}, with average of 85.4 ± 0.6% for Cd(II), 88.0 ± 0.9% for

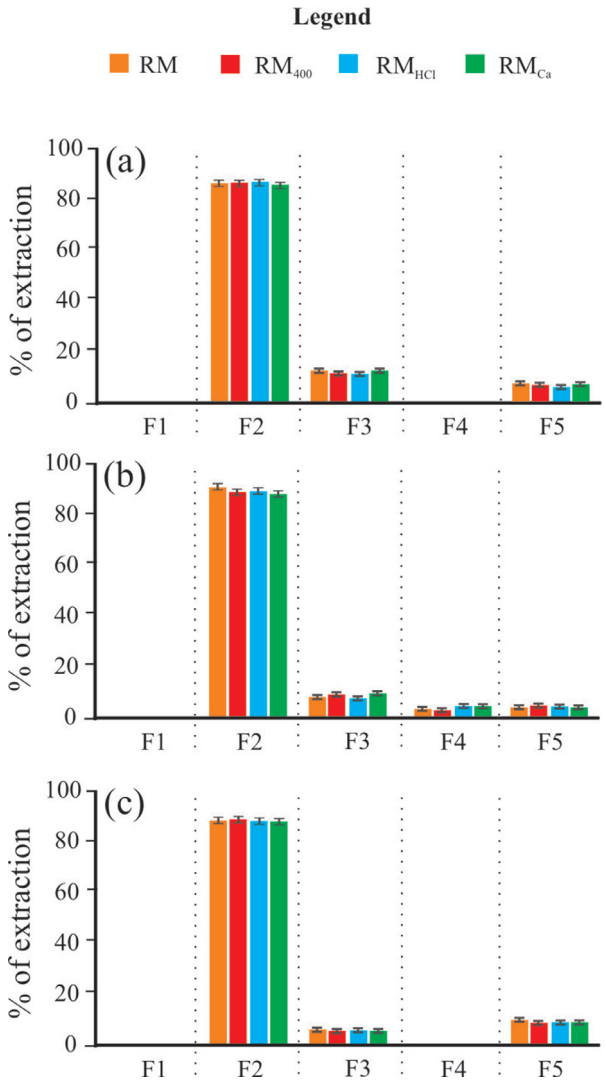

Fig. 4. Percentages of labile and residual geochemical fractions of the Cd(II) (a), Pb(II) (b) and Zn(II) (c), using RM, RM_{400}, RM_{HCl} and RM_{Ca} (C_0 = 2 mmol 25 mL^{-1}). The experiment was performed in triplicate; with the bars indicate standard deviation.

Pb(II) and 87.7 ± 0.4% for Zn(II). Thus, the mechanism related to Cd(II), Pb(II) and Zn(II) removal from aqueous solution in the natural and activated RM can be truly associated with these trace elements bound to carbonate. Similar results have also shown that carbonate is the main labile fraction responsible for Cu(II) (Qi et al., 2018) removal from aqueous solution by natural RM collected from Shanxi in China, respectively. Even without a sequential extraction study, Lyu et al. (2020) showed that the precipitation processes, as Pb-carbonates, was responsible for 78% of Pb(II) removal from aqueous solution by modified RM (colloidal silica and sodium hydroxide).

3.3. Mechanisms of Cd(II), Pb(II) and Zn(II) removal by mineral precipitation

During the sequential extractions, the lower removal percentages for Cd(II), Pb(II) and Zn(II) were detected in the ion exchangeable fractions (< 0.4% for all trace elements), whereas the higher percentages were bound to carbonate fraction. This suggest the mineral precipitation as the main mechanisms of Cd(II), Pb(II) and Zn(II) removal instead of adsorption onto sodalite. Therewith, adsorption Langmuir and Freundlich

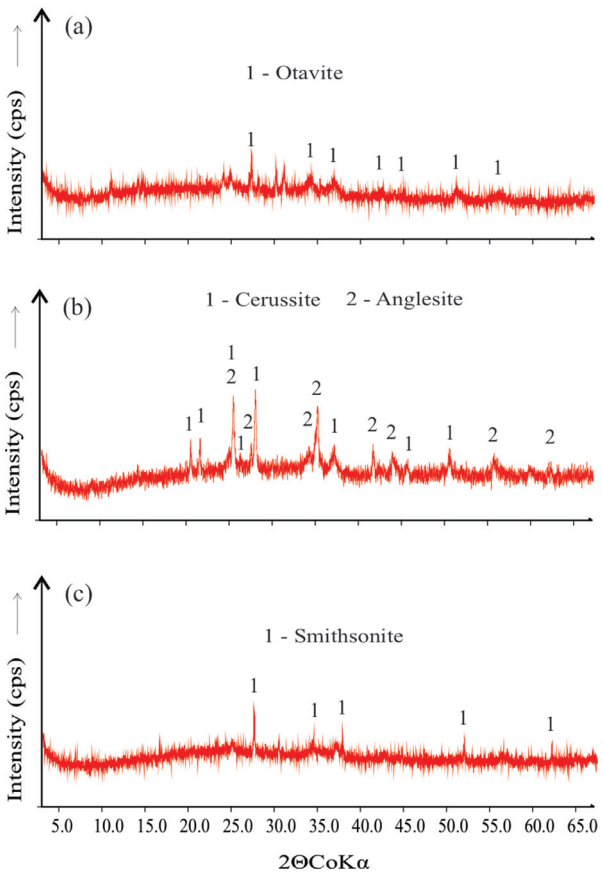

Fig. 5. The RM_{400} XDR patterns after Cd(II) (a), Pb(II) (b) and Zn(II) (c) removal experiments.

isotherms are not valid to model the Cd(II), Pb(II) and Zn(II) removal using these hazardous materials.

Mann and Deutscher (1980) studied the Pb(II) and Zn(II) mobility in water containing carbonate, sulphate and chloride ions. Sangameshwar and Barnes (1983) assessed thermodynamically the distribution and stabilities of mineral assemblages formed in system with Cd(II), Pb (II) and Zn(II)+CO_2+S+H_2O at 25 °C and 1 atm, with Eh-pH diagrams illustrating clearly that the mineral assemblages depends on the Eh and pH conditions. At the pH values used in the experimental procedures (initial of 7 and final of 5), the natural and activated forms of RM in solutions with pH values lower than the pH_{PCZ} developed a positive charge on their surface, when pH values were lower than the pH_{PCZ}. This result in the elestrostatic repulsion exists between the positively charged surface of the RM and the cationic ions, such as Cd(II), Pb(II) and Zn(II).

Considering the initial and final pH values, the Eh-pH diagrams proposed by Sangameshwar and Barnes (1983) and the pH_{PCZ} values in the natural and activated forms of RM, the main mechanisms of Cd(II), Pb(II) and Zn(II) removal by mineral precipitation, forming otavite, cerussite, smithsonite and anglesite. Fig. 5 illustrates the RM_{400} XRD patterns after Cd(II), Pb(II) and Zn(II) removal experiment, confirming the mineral assemblages proposed. Fig. 6 presents the reaction products during the interaction bettwen Cd(II), Pb(II) and Zn(II) and RM_{Ca} in the aqueous solutions. The mineral precipitation processes can be described as following:

(a) When RM, RM_{400}, RM_{HCl} and RM_{Ca} are added in the aqueous solution with Cd(II), Pb(II) and Zn(II) at pH 7, these trace elements react with HCO_3^- available in the natural and activated forms of RM, producing Cd(II), Pb(II) and Zn(II) precipitates, such as otavite (Eq. (4)), cerussite (Eq. (5)) and smithsonite (Eq. (6));

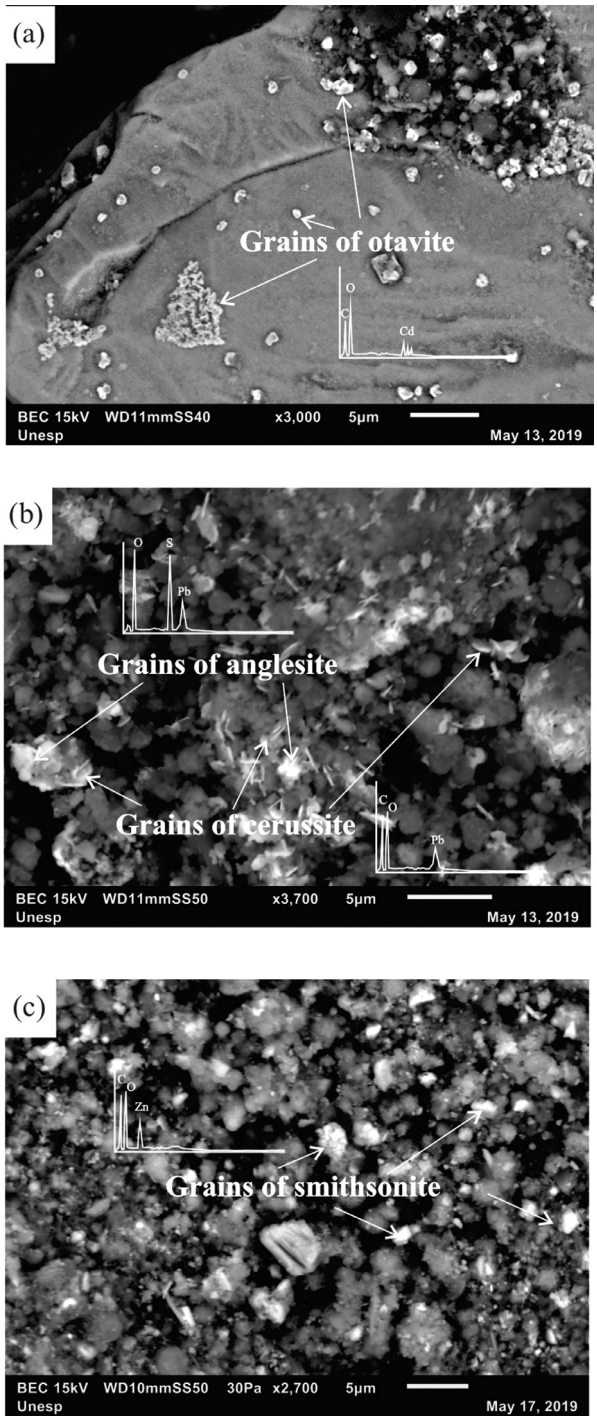

Fig. 6. Reaction products during the interaction bettwen Cd(II) (a), Pb(II) (b) and Zn(II) (c) in the aqueous solutions and RM.

$$Cd^{2+} + HCO_3^- \rightarrow CdCO_3\ (otavite) + H^+ \quad (4)$$

$$Pb^{2+} + HCO_3^- \rightarrow PbCO_3\ (cerussite) + H^+ \quad (5)$$

$$Zn^{2+} + HCO_3^- \rightarrow ZnCO_3\ (smithsonite) + H^+ \quad (6)$$

(b) For natural and activated forms of RM, with the total consumption of HCO_3^- and production of H^+, the pH values decreased and Pb(II) precipitates as anglesite (Eq. (7)) at pH values below 5.4 (Sangameshwar and Barnes, 1983; Marani et al., 1995). The anglesite precipitation explains the Pb(II) removal percentages in the bound to organic matter/sulfide (2.8 ± 0.2%);

$$Pb^{2+} + S^{2-} + 4H_2O \rightarrow PbSO_4\ (anglesite) + 8H^+ \quad (7)$$

(c) Greenockite or hawleyite (CdS), galena (PbS) and sphalerite (ZnS) are not precipitated due to oxidation conditions during the Cd(II), Pb(II) and Zn(II) removal experiments.

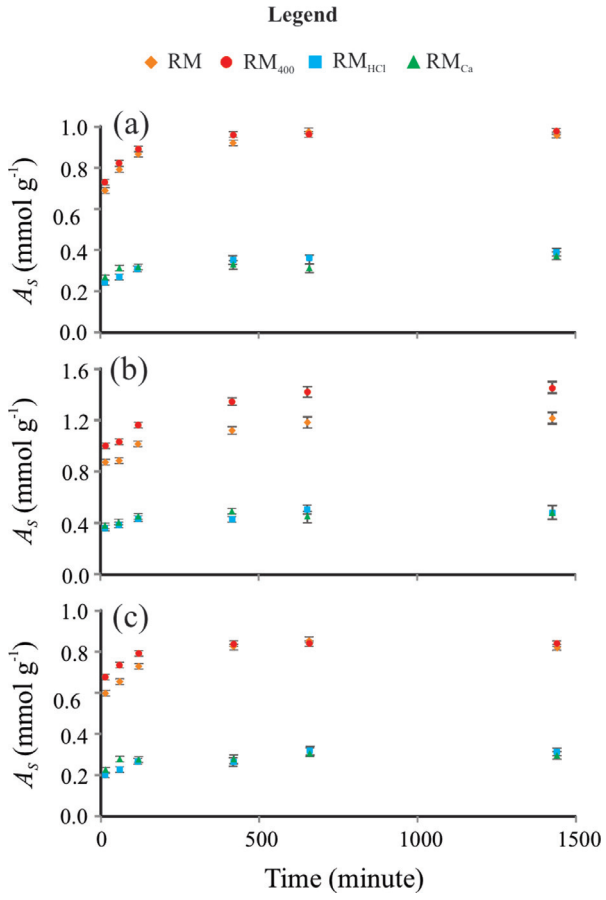

Fig. 7. Removal efficiency (*RE*) of the Cd(II) (a), Pb(II) (b) and Zn(II) (c) versus time, using RM, RM_{400}, RM_{HCl} and RM_{Ca} (C_0 = 80 mmol L^{-1}). The experiment was performed in triplicate; with the bars indicate standard deviation.

3.4. Kinetics study of Cd(II), Pb(II) and Zn(II) removal

Fig. 7 shows the A_s values (Eq. (2)) over time for the Cd(II) Pb(II) and Zn(II) removal onto RM, RM_{400}, RM_{HCl} and RM_C. The Cd(II), Pb(II) and Zn(II) removal depends on the reaction time and either natural and activated RM is used. In the first 15 min, ca. 70% of Cd(II), Pb(II) and Zn(II) was removed. In addition, Cd(II), Pb(II) and Zn(II) removal trend to their maximum after 120 min (2 h) for all tested RM variants. The maximum amount of trace elements removed using RM, RM_{400}, RM_{HCl} and RM_{Ca} were 0.95, 0.99, 0.37 and 0.35 and mmol g^{-1} for Cd(II), 1.27, 1.39, 0.51 and 0.50 mmol g^{-1} for Pb(II) and 0.90, 0.94, 0.28 and 0.30 mmol g^{-1} for Zn(II), respectively, after 1440 min (24 h). Different RM removal capacities has been described in the literature for Cd(II), Pb(II) and Zn(II) (Table 1), as a consequence of not only the large minerals variability, but also the specific surface area, chemical composition and activation procedures as well (Wang et al. 2008).

The thermal treatment promoted the transformation of goethite and gibbsite into hematite and alumina and consequently, promoting the increment in the SSA in the RM_{400} (61 $m^2\ g^{-1}$) when compared to RM (33 $m^2\ g^{-1}$). Antunes et al. (2012) proposed that the thermal treatment

at 400–500 °C would be the best temperature to increase the SSA and, consequently, the adsorption associated with new mineral phases generated (hematite and alumina). In addition, the pH values were practically the same for the RM (10.5) and RM_{400} (10.7), indicating that the thermal treatment did not remove the HCO_3^- available in these materials. Thus, the increment in the SSA and, consequently, in the reactive -OH and -OH_2 functional groups exposed on the RM_{400} surface (Liu and Huang, 2003), increases the Cd(II), Pb(II) and Zn(II) removal onto the Fe-Mn oxides compared to RM.

On the other hand, the chemical treatment with HCl and $Ca(NO_3)_2$ decreased the Cd(II), Pb(II) and Zn(II) removal efficacy in ca. 60% in relation to RM. This fact was also described by Santona et al. (2006), Pichinelli et al. (2017) and Silva et al. (2019), who suggested that the chemical treatments dissolved a portion of the zeolite-types minerals, reducing the trace elements removal capacity. However, our study showed clearly the Cd(II), Pb(II) and Zn(II) removal on the activated forms of RM is associated to chemical treatment used to activate RM_{HCl} and RM_{Ca} samples. This cause the reduction of the amount HCO_3^- available in solution and the consequent limitation to a minimum residual fractions in solution for Cd(II), Pb(II) and Zn(II).

Kinetics models were made to describe the sorption of pollutants on solid surfaces for liquid-solid phase sorption systems (Ho and McKay, 1998), such as the pseudo-first-order Lagergren, pseudo-second-order, Elovich and intraparticle diffusion models. These traditional kinetics models have been used to study the removal of several trace elements using natural or activated RM (López et al., 1998; Gupta et al., 2001; Gupta and Sharma, 2002; Sahu et al., 2011; Pichinelli et al., 2017; Silva et al., 2019; Yang et al., 2020; Lyu et al., 2020). However, considering the central role of mineral precipitation mechanism on trace elements removal, the traditional kinetics models commonly associated to trace elements adsorption by RM should applied carefully, once may not represent the mineral precipitation phenomenon.

3.5. Modelling Cd(II), Pb(II) and Zn(II) removal by carbonate precipitation

Precipitation was the main responsible for removal of ca. 85% for Cd(II), Pb(II) and Zn)II), as seen in sequential extractions experiment. Considering Greenberg and Tomson (1992), we assumed the kinetic reaction of n^{th} order as plausible to explain the behaviour of metals decay. To perform the model, we used n of the n^{th} order reaction as one of the adjusting parameters, along with the kinetic constant. According to the pH values using during the kinetics studies, the precipitation kinetic was considered to depend upon the trace elements and RM concentrations, and the availability of HCO_3^- in solution, for a given pH and PCO_2. Eq. (8) shows a general derivative form for a second order reaction.

$$\frac{d[A]}{dt} = -k[A].[B].PCO_2 \quad (8)$$

where:

k = precipitation rate constant for partial pressure of CO_2 at 25 °C (mmol L^{-1} min^{-1}) $(atm)^{-1}$; $[A]$ = concentration of the trace element in solution at time (t) (mmol L^{-1}); $[B]$ = concentration of HCO_3^- derived of the natural or activated RM in solution at time (t) (mmol L^{-1}); PCO_2 = partial pressure of CO_2 due to pH at 25 °C (atm).

Assuming $[B] \approx [A]$ and integrating from initial concentration to the concentration at time t, then Eq. (8) yields Eq. (9).

$$[A] = \left([A_0]^{-n+1} + (n-1).k'.t \right)^{-\frac{1}{n-1}} + k_C \quad (9)$$

where:

$[A_0]$ = concentration of $[A]$ in solution at time (t) zero (mmol L^{-1}); n = n^{th} general reaction order; k' = precipitation rate constant (mmol L^{-1} min^{-1}), k_c = constant applied to take into account the limited capacity of HCO_3^- transfer from natural or activated RM to solution (mmol L^{-1}), describing the asymptotic limit for the trace elements precipitation due to HCO_3^- availability in solution.

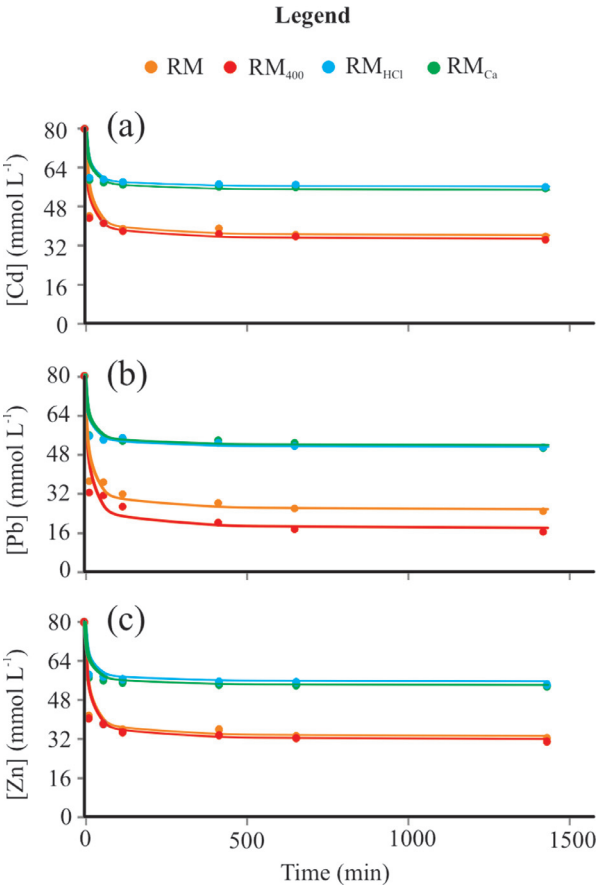

Fig. 8. Kinetics of Cd(II) (a), Pb(II) (b) and Zn(II) (c) precipitation, using RM, RM_{400}, RM_{HCl} and RM_{Ca}, considering C_0 = 80 mmmol L^{-1} and Cd(II), Pb(II) and Zn(II) removal by carbonate precipitation in ca. 85%. Symbols are experimental data.

Table 3
Parameters obtained for the modelling Pb(II) and Zn(II) removal by precipitation.

Element RM	k' (mmol L^{-1} min^{-1})	k_c (mmol L^{-1})	R^2
Cd(II)	0.32	35.6	0.99
Pb(II)	0.44	24.8	0.98
Zn(II)	0.32	37.6	0.98
RM_{400}			
Cd(II)	0.32	34.4	0.99
Pb(II)	0.48	20.4	0.96
Zn(II)	0.32	32.0	0.99
RM_{HCl}			
Cd(II)	0.12	55.6	0.99
Pb(II)	0.16	50.8	0.99
Zn(II)	0.08	58.4	0.99
RM_{Ca}			
Cd(II)	0.12	56.0	0.99
Pb(II)	0.16	51.2	0.98
Zn(II)	0.12	57.6	0.99

The Cd(II), Pb(II) and Zn(II) precipitation mechanisms using natural or activated forms of RM was modelled using Eq. (9) (Fig. 8). The parameters (k', kc and n) of Eq. 9 were calculated by minimising the sum of the squared difference between experimental and modelled data, using non-linear generalized reduced gradient algorithm of SOLVER - MS Excell®. Table 3 shows results obtained for Eq. (9) parameters and R^2 as well. The results showed the second order reaction as the best trend line for Cd(II), Pb(II) and Zn(II) precipitation, with R^2 higher than 0.96 for all trace elements. The second order reaction are in accordance with

data reported in literature (e.g., Gilmour et al., 1977; Kazmierczak et al., 1981, Greenberg and Tomson, 1992). The proposed constant k_c limit precipitation accordingly, as HCO_3^- concentration in solution decay over time.

The average Cd(II), Pb(II) and Zn(II) precipitation rates constants were 0.36, 0.40, 0.12 and 0.13 (mmol L^{-1} min^{-1}) for RM, RM_{400}, RM_{HCl} and RM_{Ca}, respectively. The kinetics of these trace elements precipitation showed fast removal within the first 15 min, with little increment of the Cd(II), Pb(II) and Zn(II) removal by precipitation as carbonates by HCO_3^- and H_2CO_3 equilibrium. In addition, the Cd(II), Pb(II) and Zn(II) removal by mineral precipitation is a typical biphasic precipitation kinetics for all natural and activated forms RM, with a fast trace elements precipitation within the first 120 min, followed by steady of these trace elements removal. In the fast precipitation kinetics, mainly due to Cd(II), Pb(II) and Zn(II) precipitation with HCO_3^- available in the aqueous solution, provides a rapid decrease in the HCO_3^- concentration. This fact limits the Cd(II), Pb(II) and Zn(II) removal by mineral precipitation from 120 to 1440 min because the less HCO_3^- available for the formation of otavite, cerussite, smithsonite and anglesite in the natural and activated forms of RM.

Summarizing, under the experimental conditions herein presented, both selective extraction and kinetics study have shown that carbonate precipitation is the most relevant mechanism for Cd(II), Pb(II) and Zn(II) removal using RM, RM_{400}, RM_{HCl} and RM_{Ca} from aqueous solutions, regardless the natural and activated forms of RM, and that the of HCO_3^- plays a crucial role in kinetics by limiting the precipitate formation.

4. Conclusions

The Cd(II), Pb(II) and Zn(II) removal mechanisms from aqueous solution using natural and different chemical (HCl 0.05 mol L^{-1} and $Ca(NO_3)_2$ 0.1 mol L^{-1}) and thermal (400 °C) RM were studied using sequential extraction. In addition, the kinetics of Cd(II), Pb(II) and Zn(II) removal by carbonate precipitations were modelled. Results showed the carbonate fraction was the main labile fraction responsible for the higher Cd(II), Pb(II) and Zn(II) removal percentages (ca. 85%), followed by bound Fe-Mn oxides, bound to organic matter/sulphide and ion exchangeable fractions. Irrespective of whether natural and activated forms of RM, the mineral precipitation was the main mechanism for Cd(II), Pb(II) and Zn(II) removal, forming otavite – $CdCO_3$, cerussite - $PbCO_3$, smithsonite - $ZnCO_3$ and anglesite - $PbSO_4$. Kinetics studies showed a maximum amount of trace elements removed using RM, RM_{400}, RM_{HCl} and RM_{Ca} of 0.95, 0.99, 0.37 and 0.35 and mmol g^{-1} for Cd(II), 1.27, 1.39, 0.51 and 0.50 mmol g^{-1} for Pb(II) and 0.90, 0.94, 0.28 and 0.30 mmol g^{-1} for Zn(II). These results clearly indicated that the chemical treatments decreased the Cd(II), Pb(II) and Zn(II) removal whilst the thermal treatments increased up to 10% the trace elements removal in relation to RM. Therefore, chemical and thermal treatments do not bring a relevant improvement for trace elements removal and they can be avoided, lowering the costs associated to these procedures. A fast trace elements precipitation occurred within the first 120 min, with limitation in these trace elements removal due to HCO_3^- consumption during the mineral precipitation. Consequently, the traditional adsorption isotherms and kinetics models commonly associated to trace elements adsorption by RM should be considered carefully in future studies. As a whole, the results provide new insights into the relative importance of the Cd(II), Pb(II) and Zn (II) removal mechanisms from aqueous solution using natural and activated forms of RM. Furthermore, the results pointed out to the use of these hazardous materials on environmental systems in the framework of environmental remediation and water industry in areas heavily impacted by anthropogenic activities. It should be underscored that the residual RM should be properly stored, in order to prevent the solubilization of the labile fraction of trace elements to the environment, especially for the labile trace elements fractions. Future studies applicable to use of RM on a larger scale and for reuse of Cd(II), Pb(II) and Zn(II) precipitated in the industrial activities are advised.

Declaration of Competing Interest

The authors declare that they have no known competing financial interests or personal relationships that could have appeared to influence the work reported in this paper.

Acknowledgment

The authors thank the Fundação de Amparo à Pesquisa do Estado de São Paulo (FAPESP - Processes No. 2009/02374-0 and 2013/00994-6) and Conselho Nacional de Desenvolvimento Científico e Tecnológico (CNPq - Process No. 480555/2009-5) for financial support. Dr. Moruzzi is also grateful to CNPq for grant awarded 301210/2018-7. We thank all the referees for their detailed and insightful review's comments, whom helped to improve the manuscript.

References

Amazônia Real, 2018. Vazamento de rejeitos da Hydro Alunorte causa danos socioambientais em Barbacena.https://amazoniareal.com.br/vazamento-de-rejeitos-da-hydro-alunorte-causa-danos-socioambientais-em-barcarena-no-para/ (accessed 9 November 2020).

Antunes, M.L.P, Couperthwaite, S.J., Conceição, F.T., Jesus, C.P.C., Kiyohara, P.K., Coelho, A.C.V., Frost, R.L., 2012. Red mud from Brazil: thermal behaviour and physical properties. Ind. Eng. Chem. Res. 51, 775–779. doi:10.1021/ie201700k.

Apak, R., Guclu, K., Turgut, M.H., 1998a. Modelling of copper (II), cadmium (II) and lead (II) adsorption on red mud. J. Colloid Interface Sci. 203, 122–130. doi:10.1006/jcis.1998.5457.

Apak, R., Tütem, E., Hügül, M., Hizal, J., 1998b. Heavy metal cation retention by unconventional sorbents (red muds and fly ashes). Water Res. 32, 430–440. doi:10.1016/S0043-1354(97)00204-2.

Ayala, J., Fernandez, B., 2019. Removal of zinc, cadmium and nickel from mining waste leachate using walnut shells. Environ. Prot. Eng. 45, 141–158. doi:10.5277/epe190210.

Brasil, 2018. Sumário Mineral. Departamento Nacional de Produção Mineral (DNPM), Brasília.

Conceição, F.T., Pichinelli, B.C., Silva, M.S.G., Moruzzi, R.B., Menegário, A.A., Antunes, M.L.P., 2016. Cu(II) adsorption from aqueous solution using red mud activated by chemical and thermal treatment. Environ. Earth Sci. 75, 362. doi:10.1007/s12665-015-4929-y.

Fortes, G.M., Lourenço, R.R., Montini, M., Gallo, J.B., Rodrigues, J.A., 2016. Synthesis and mechanical characterization of iron oxide rich sulfobelite cements prepared using bauxite residue. Mater. Res. 19, 276–284. doi:10.1590/1980-5373-MR-2015-0180.

Gilmour, J.T., Shirk, J.A., Fergunson, J.A., Griffis, C.L., 1977. A kinetic study of the $CaCO_3$ precipitation reaction. Agric. Water Manag. 1, 253–262. doi:10.1016/0378-3774(77)90004-X.

Greenberg, J., Tomson, M., 1992. Precipitation and dissolution kinetics and equilibria of aqueous ferrous carbonates *vs* temperature. Appl. Geochem. 7, 185–190. doi:10.1016/0883-2927(92)90036-3.

Gupta, V.K., Gupta, M., Sharma, S., 2001. Process development for the removal of lead and chromium from aqueous solutions using red mud – an aluminum industry waste. Water Res. 35, 1125–1134. doi:10.1016/S0043-1354(00)00389-4.

Gupta, V.K., Sharma, S., 2002. Removal of cadmium and zinc from aqueous solutions using red mud. Environ. Sci. Technol. 36, 3612–3617. doi:10.1021/es020010v.

Hind, A.R., Bhargava, S.K., Grocott, S.C., 1999. The surface chemistry of Bayer process solids: a review. Colloids Surf. A 146, 359–374. doi:10.1016/S0927-7757(98)00798-5.

Ho, Y.S., Mckay, G., 1998. A comparison of chemisorption kinetic models applied to pollutant removal on various sorbents. Trans. Inst. Chem. Eng. 76, 332–340. doi:10.1205/095758298529696.

Hua, Y., Heal, K.V., Friesl-Hanl, W., 2017. The use of red mud as an immobiliser for metal/metalloid-contamined soil: a review. J. Hazard. Mater. 325, 17–30. doi:10.1016/j.jhazmat.2016.11.073.

Jesus, C.P.C, Antunes, M.L.P., Concieção, F.T, Navarro, G.R.B., Moruzzi, R.B., 2015. Removal of reactive dye from aqueous solution using thermally treated red mud. Desalin. Water Treat. 55, 1040–1047. doi:10.1080/19443994.2014.922444.

Jones, B.E.H., Haynes, R.J., 2011. Bauxite processing residue: a critical review of its formation, properties, storage, and revegetation. Crit. Rev. Environ. Sci. Technol. 41, 271–315. doi:10.1080/10643380902800000.

Kazmierczak, T.F., Schuttringer, E., Tomazic, B., Nancollas, G.H., 1981. Controlled composition studies of calcium carbonate and sulfate crystal growth. Croat. Chem. Acta 54, 277–287.

Leleyter, L., Probst, J.L., 1999. A new sequential extraction procedure for the speciation of particulate trace elements in river sediments. Int. J. Environ. Anal. Chem. 73, 109–128. doi:10.1080/03067319908032656.

Liu, C., Huang, P.M., 2003. Kinetics of lead adsorption by iron oxides formed under the influence of citrate. Geochim. Cosmochim. Acta 67, 1045–1054. doi:10.1016/S0016-7037(02)01036-0.

López, E., Soto, B., Arias, M., Nunez, A., Rubinos, D., Barral, M.T., 1998. Adsorbent properties of red mud and its use for wastewater treatment. Water Res. 32, 1314–1322. doi:10.1016/S0043-1354(97)00326-6.

Lyu, F., Niu, S., Wang, L., Sun, W., He, D., 2020. Efficient removal of Pb(II) ions from aqueous solution by modified red mud. J. Hazard. Mater. 15, 124678. doi:10.1016/j.jhazmat.2020.124678.

Mann, A.W., Deutscher, R.L., 1980. Solution geochemistry of lead and zinc in water containing carbonate, sulphate and chloride ions. Chem. Geol. 29, 293–311. doi:10.1016/0009-2541(80)90026-1.

Marani, D., Macchi, G., Pagano, M., 1995. Lead precipitation in the presence of sulphate and carbonate: testing of thermodynamic predictions. Water Res. 29, 1085–1092. doi:10.1016/S0043-1354(94)00232-V.

Mon, J., Deng, Y., Flury, M., Harsh, J.B., 2005. Cesium incorporation and diffusion in cancrinite, sodalite, zeolite, and allophone. Microporous Mesoporous Mater. 86, 277–286. doi:10.1016/j.micromeso.2005.07.030.

Nadaroglu, H., Kalkan, E., Demir, N., 2010. Removal of copper from aqueous solution using red mud. Desalination 251, 90–95. doi:10.1016/j.desal.2009.09.138.

Órfão, J.J.M., Silva, A.I.M., Pereira, J.C.V., Barata, S.A., Fonseca, I.M., Faria, P.C.C., Pereira, M.F.R., 2006. Adsorption of reactive dye on chemically modified activated carbons – influence of pH. J. Colloid Interface Sci. 296, 480–489. doi:10.1016/j.jcis.2005.09.063.

Pichinelli, B.C., Silva, M.S.G., Conceição, F.T., Menegario, A.A., Antunes, M.L.P., Navarro, G.R.B., Moruzzi, R.B., 2017. Adsorption of Ni(II), Pb(II) and Zn(II) on $Ca(NO_3)_2$-neutralised red mud. Water Air Soil Pollut. 228, 1–13. doi:10.1007/s11270-016-3208-1.

Pulford, I.D., Hargreaves, J.S.J., Durisová, J., Kramulova, B., Girard, C., Balakrishnan, M., Batra, V.S., Rico, J.L., 2012. Carbonised red mud - a new water treatment product made from a waste material. J. Environ. Manag. 100, 59–64. doi:10.1016/j.jenvman.2011.11.016.

Qi, X., Wang, H., Huang, C., Zhang, L., Zhang, J., Xu, B., Li, F., Junior, J.T.A., 2018. Analysis of bauxite residue components responsible for copper removal and related reaction products. Chemosphere 207, 209–217. doi:10.1016/j.chemosphere.2018.05.041.

Qi, X., Wang, H., Zhang, L., Xu, B., Shi, Q., Li, F., 2020. Removal of Cr (III) from aqueous solution by using bauxite residue (red mud): identification of active components and column tests. Chemosphere 245, 125560. doi:10.1016/j.chemosphere.2019.125560.

Sahu, R.C., Patel, R., Ray, B.C., 2011. Adsorption of Zn(II) on activated red mud: Neutralized by CO_2. Desalination 266, 93–97. doi:10.1016/j.desal.2010.08.007.

Sangameshwar, S.R., Barnes, H.L., 1983. Supergene processes in zinc-lead-silver sulfide ores in carbonates. Econ. Geol. 78, 1379–1397. doi:10.2113/gsecongeo.78.7.1379.

Santona, L., Castaldi, P., Melis, P., 2006. Evaluation of the interaction mechanisms between red mud and heavy metals. J. Hazard. Mater. 136, 324–329. doi:10.1016/j.jhazmat.2005.12.022.

São Paulo, Companhia Ambiental do Estado de São Paulo, 2012. Ficha de Informação Toxicológica. http://www.cetesb.sp.gov.br/userfiles/file/laboratorios/fit/cobre.pdf (accessed 12 September 2012).

Silva, M.S.G., Pichinelli, B.C., da Conceição, F.T., Moruzzi, R.B., Yabuki, L.N., Menegário, A.A., Antunes, M.L.P., 2019. Adsorção de Cd (II) por lama vermelha natural e com diferentes ativações. Geochim. Bras. 33, 76–88 http://dx.doi.org/10.21715/GB2358-2812.2019331076.

Silva Filho, E.B., Alves, M.C.M., Motta, M., 2007. Lama vermelha da indústria de beneficiamento de alumina: produção, características, disposição e aplicações alternativas. Matéria 12, 322–338 http://dx.doi.org/10.1590/S1517-70762007000200011.

Smiciklas, I., Smiljanic, S., Peric-Grujic, A., Šljivic-Ivanovic, M., Mitric, M., Antonovic, D., 2014. Effect of acid treatment on red mud properties with implications on Ni(II) sorption and stability. Chem. Eng. J. 242, 27–35. doi:10.1016/j.cej.2013.12.079.

Smiljanic, S., Smiciklas, I., Peric-Grujic, A., Loncar, B., Mitri, M., 2010. Rinsed and thermally treated red mud sorbents for aqueous Ni^{2+} ions. Chem. Eng. J. 162, 75–83. doi:10.1016/j.cej.2010.04.062.

Souza, K.C., Antunes, M.L.P., Couperthwaite, S.J., Conceição, F.T., Barrs, T.R., Frost, R., 2013. Adsorption of reactive dye on seawater-neutralised bof reactive dye on seawater-neutralised bauxite refinery residue. J. Colloid Interface Sci. 396, 210–214. doi:10.1016/j.jcis.2013.01.011.

Tessier, A., Campbell, P.G.C., Bisson, M., 1979. Sequential extraction procedure for the speciation of particulate trace metals. Anal. Chem. 51, 844–851. doi:10.1021/ac50043a017.

USEPA, 1990. Methods for Chemical Analysis of Water and Wastes EPA 3010 Cincinnati, Ohio.

Vaclavikova, M., Misaelides, P., Gallios, G., Jakabsky, S., Hredzak, S., 2005. Removal of cadmium, zinc, copper and lead by red mud, an iron oxides containing hydrometallurgical waste. Stud. Surf. Sci. Catal. 155, 517–525. doi:10.1016/S0167-2991(05)80179-X.

Wang, S., Ang, H.M., Tadé, M.O., 2008. Novel applications of red mud as coagulant, adsorbent and catalyst for environmentally benign processes. Chemosphere 72, 1621–1635. doi:10.1016/j.chemosphere.2008.05.013.

Whittington, B.I., Fletcher, B.L., Talbot, C., 1998. The effect of reaction conditions on the composition of desilication product (DSP) formed under simulated Bayer conditions. Hydrometallurgy 49, 1–22. doi:10.1016/S0304-386X(98)00021-8.

Yang, T., Wang, Y., Sheng, L., He, C., Sun, W., He, Q., 2020. Enhancing Cd(II) sorption by red mud with heat treatment: performance and mechanism of sorption. J. Environ. Manage. 255, 109866. doi:10.1016/j.jenvman.2019.109866.